DOI: https://doi.org/10.37434/tpwj2023.10.07

NUMERICAL-INSTRUMENTAL METHOD OF THERMOGRAPHIC CONTROL OF THE STATE OF LARGE-SIZED STRUCTURES AND CONSTRUCTIONS

O.S. Milenin, V.Yu. Glukhovskyi, O.A. Velykoivanenko, V.A. Lytvynenko

E.O. Paton Electric Welding Institute of the NASU
11 Kazymyr Malevych Str., 03150, Kyiv, Ukraine

ABSTRACT

A numerical-instrumental approach of thermographic control was developed to improve the efficiency of contactless control of the state of difficult-of-access parts of large-sized structures and constructions. It consists in integrated application of industrial thermal imaging instruments and computational methods of analysis of temperature fields in the studied structures. This allows improving the accuracy of determination of the geometrical features of the defects and reducing the labour consumption of operations of technical diagnostics of the state. Application of the developed approach was demonstrated on typical examples of contactless control of the technical state of industrial chimneys.

KEYWORDS: thermographic control, technical state, flaw detection, industrial chimneys, heat transfer

INTRODUCTION

Diagnostics of the technical state of large-sized structures, buildings and constructions of long-term operation is a mandatory stage of expert analysis of their state and the basis for planning measures of repair and restoration works. One of the main aspects of the study is to detect defects in structures that can affect the integrity and functionality of the corresponding structural components.

To analyse structures of a certain class (residential and non-residential buildings, chimneys, tanks, high-pressure vessels) while detecting geometric anomalies of different types, the methods of passive thermographic control (TC) proved to be efficient, which allow diagnosing the state of buildings in difficult-of-access places avoiding the use of the high-cost equipment and reducing production risks for staff [1, 2]. The essence of this method consists in the fact that the temperature difference inside the examined structure and outside is different, and it causes a certain heating of the outer surface. The actual distribution of surface temperature depends on many factors, in particular, on thermal resistance of a structure, heat conductivity of materials, as well as on the presence of operation defects, i.e. local thinning or cavities in the wall. This can be registered using contactless thermographic methods. The simplicity and availability of this approach caused its widespread use for the assessment of thermal characteristics of buildings, detection of zones of excessive heat losses, air leaks, absence or failure to thermal insulation, moisture sources, etc. [3, 4]. The contactless nature of TC allows it to be widely used to analyze the failure to metal materials, as well as to detect subsurface defects in polymers or composites [5, 6].

However, one of the fundamental disadvantages of this method of technical diagnostics is the low accuracy of quantitative assessment of sizes of detected defects, especially over the thickness of a structure. This means that in case of detection of certain anomalies, in order to prepare the reasonable expert opinion about their admissibility, additional measures are necessary to inspect the corresponding structural element, which, in some way, diminishes the benefits of TC. Therefore, the development of science-intensive approaches to the analysis of the results of measuring temperature fields in terms of quantitative interpretation is relevant.

THE AIM

of the work is the development of a numerical-instrumental method of TC of the state of large-sized structures and constructions on the basis of integrated use of thermal imaging instruments and computational approaches for thermal fields analysis.

RESEARCH PROCEDURE

The instrumental part of the proposed procedure consists in the thermographic measurement of natural (passive thermography) or induced (active thermography) fields on the surface of plane or cylindrical structures. The areas of surface or subsurface defects are characterized by change in the local temperature. In this case, the ratio of temperatures in the area of a defect and in the defect-free area of the structure depends, first of all, on the residual thickness of the wall and the type of a defect. To determine the type (surface, subsurface) and the actual size of discontinuity, it is necessary to know the dependences of the local temperature on the outer surface of the structure in the area of a defect on the thermophysical properties of the material and the features of the temperature effect. Such dependencies were obtained on the basis of a numerical computation of the temperature field, taking into account the geometric and physical features of the structural state. Validation of mathematical models and tools for their computer implementation was conducted on the basis of appropriate laboratory studies of model structural elements.

Thus, the computation of an uneven temperature field was based on the finite-differential solution of the non-stationary heat conductivity equation [7, 8]:

● in the Cartesian coordinate system (x, y, z) — to describe the heat transfer processes in the plates:

$$C\rho(x,y,z,T)\cdot\frac{\partial T(x,y,z,t)}{\partial t}= =\frac{\partial}{\partial x}\left[\lambda(x,y,z)\cdot\frac{\partial T(x,y,z,t)}{\partial x}\right]+ +\frac{\partial}{\partial y}\left[\lambda(x,y,z)\cdot\frac{\partial T(x,y,z,t)}{\partial y}\right]+ +\frac{\partial}{\partial z}\left[\lambda(x,y,z)\cdot\frac{\partial T(x,y,z,t)}{\partial z}\right]. \tag{1}$$

● in the cylindrical coordinate system (r, β, z) — for the cylindrical structures:

$$C\rho(r,\beta,z,T)\cdot\frac{\partial T(r,\beta,z,t)}{\partial t}= =\frac{1}{r}\cdot\frac{\partial}{\partial r}\left[r\cdot\lambda(r,\beta,z)\cdot\frac{\partial T(r,\beta,z,t)}{\partial r}\right]+ +\frac{1}{r^2}\cdot\frac{\partial}{\partial\beta}\left[\lambda(r,\beta,z)\cdot\frac{\partial T(r,\beta,z,t)}{\partial\beta}\right]+ +\frac{\partial}{\partial z}\left[\lambda(r,\beta,z)\cdot\frac{\partial T(r,\beta,z,t)}{\partial z}\right]. \tag{2}$$

where T is the temperature, °C; λ is the heat conductivity, J/(m^3·s·°C); $C\rho$ is the volumetric heat capacity, J/(m^3·s·°C).

When setting the problem (1) or (2), the boundary conditions of the second order were used according to the total action of characteristic sources and heat sinks. As the main dissipative processes, convective (in accordance with the Newton–Richman's law) and radiation (according to the Stefan–Boltzman law) mechanisms were considered. The process of heating from one of the surfaces of the examined object was described by the appropriate heat flow. The numerical solution of the heat conductivity equation allowed determining both the stationary temperature distribution as well as the kinetics of temperature field development, which was important during the laboratory validation of the numerical approach.

Table 1. Dependence of thermophysical properties of St3kp (rimmed) steel on temperature [9]

T, °C	Heat conductivity, W/(m·°C)	Heat capacity, J/(kg·°C)
100	55	482
200	54	498
300	50	514
400	45	533
500	39	555
600	34	584
700	30	626

LABORATORY TESTS

The developed approach was validated by comparing the temperature fields measured by a thermal imager (TESTO 876 with resolution capacity of 320×240 pixels) on the test specimens with model surface defects, with the results of numerical computations. As the test specimens, plates of 300×200×10 and 260×125×10 mm of st3 kp (rimmed) steel were used, thermophysical properties of the material, depending on the temperature are given in Table 1. As the model defects, thinning of 160 mm length, 50 mm width at 2 and 6 mm depths and horizontal subsurface delamination (1×61×66 mm at a depth of 8 mm) (Figure 1) were considered. In the framework of laboratory tests, a method of double active thermography was used, for which on one side, the specimens were heated by an infrared source, whose power varied from 1.05 to 0.45 kW, and on the other, temperature fields were measured.

The heating of the mentioned laboratory specimens was carried out at different time intervals to provide a stationary temperature field. Thus, the heating of the plate with thinning (Figure 1, *a*) proceeded during 905 s, thermograms of temperature fields on the specimen surface at different stages (5 and 65 s) are shown in Figure 2. As is seen from the measurement results, the areas of defects of thinning are characterized by a local growth in temperature compared to the periphery from 3 to 22 °C, depending on the depth of defect and the time of heating. In contrast to the defect of thinning of the plate in case of available delamination on the surface of a laboratory specimen, a drop in a local temperature as a result of an increase in thermal resistance of the plate is observed (Figure 3). For the case that was considered in the framework of the laboratory tests (Figure 1, *b*) and heating during 47 s, the amount of a local drop in the surface temperature was about 2 °C. The comparison of experimentally measured temperature distributions with the results of computations (Figure 4) show an error of not more than 15 % both at the stage of heating as well as in a stationary mode. Such a level of accuracy is sufficient

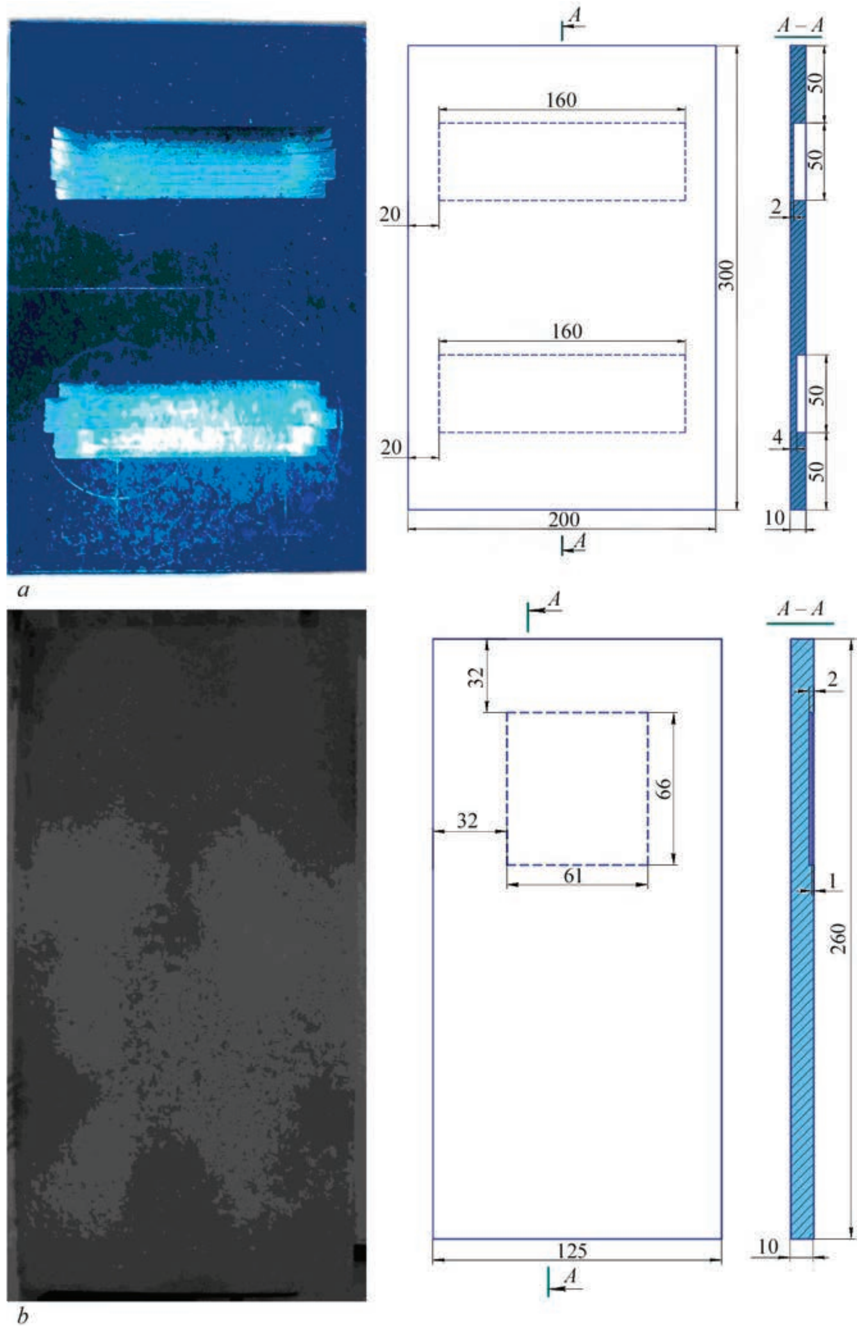

Figure 1. Appearance and schemes of plates with model defects used for laboratory tests: *a* — plate with thinning; *b* — plate with delamination

to solve engineering problems of technical diagnostics and increase the accuracy of quantitative analysis of the corresponding thermograms.

RESULTS AND DISCUSSION

The developed approach was used to increase the efficiency of diagnostics of the technical state of typical industrial chimneys on the example of structures of a reinforced concrete four-layer industrial chimney for the PTV-100 boiler units (height is 120 m, mouth diameter is 4.8 m, wall thickness of the examined area of the chimney is 0.55 m, thickness of the reinforced concrete layer is 0.120 m, brick clamping layer is 0.120 m, heat insulating layer is 0.05 m and brick lining layer is 0.120 m). Thermophysical characteristics of the layers materials are given in Table 2. Based on the results of the numerical computation, the dependences of the maximum temperature in the center of a defect of the local wall thinning from its depth and inner temperature in the chimney at different temperature of flue gases in the chimney T_{out} (Figure 5) was obtained. As is seen from this data, during failure of the inner layer of the brick lining, a rapid growth of temperature on the outer surface of the chimney begins only with the degradation of the next layer, namely thermal insulation, which imposes some restrictions on the use of TC of the technical state of such heterogeneous objects.

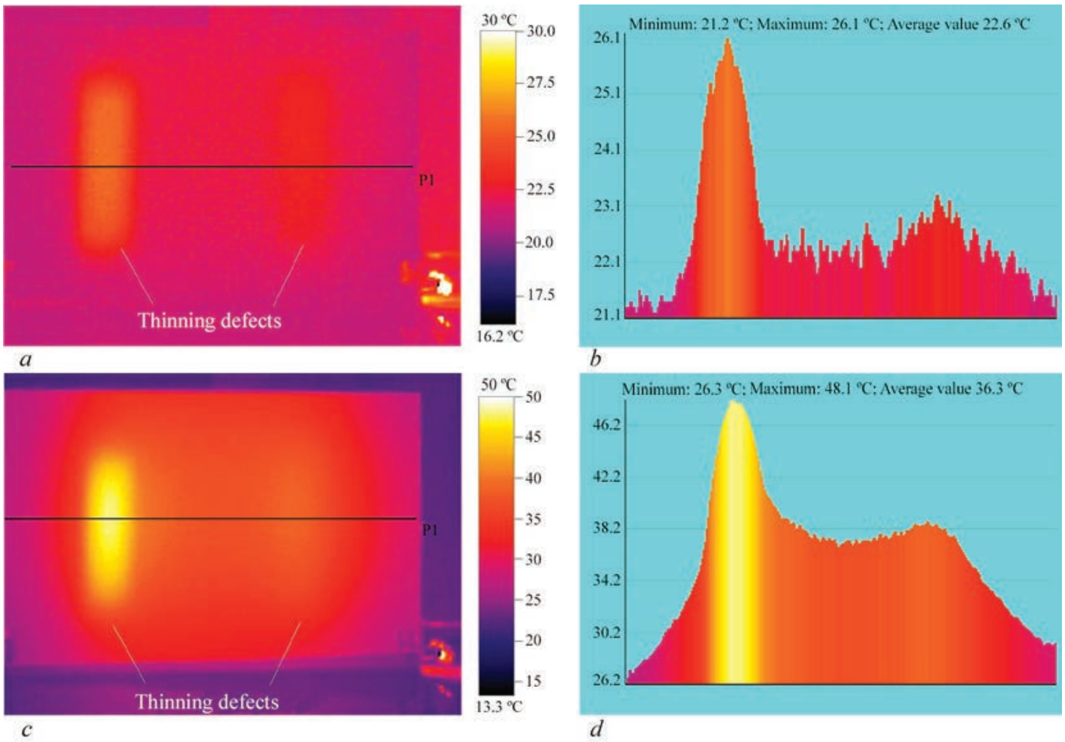

Figure 2. Thermograms of temperature fields on the surface of a plane laboratory specimen with model defects of thinning (*a*, *c*) and temperature distributions along the line P1 (*b*, *d*) at different intervals of time after the start of heating: *a*, *b* — 5 s; *c*, *d* — 65 s

With regard to subsurface delamination defects, Figure 6 shows the calculated dependences of the local temperature on radial size of a volumetric defect (size of cavity opening as a result of material degradation) located in the central insulating layer of the chimney and the temperature of flue gases. As is seen from this data, the recommended TC method is sufficiently sensitive to detect such kind of inner defects which are difficult to detect by other means of non-destructive testing: temperature difference on the surface depending on the size of a defect reaches 0.2 °C, which can be detected, tak-

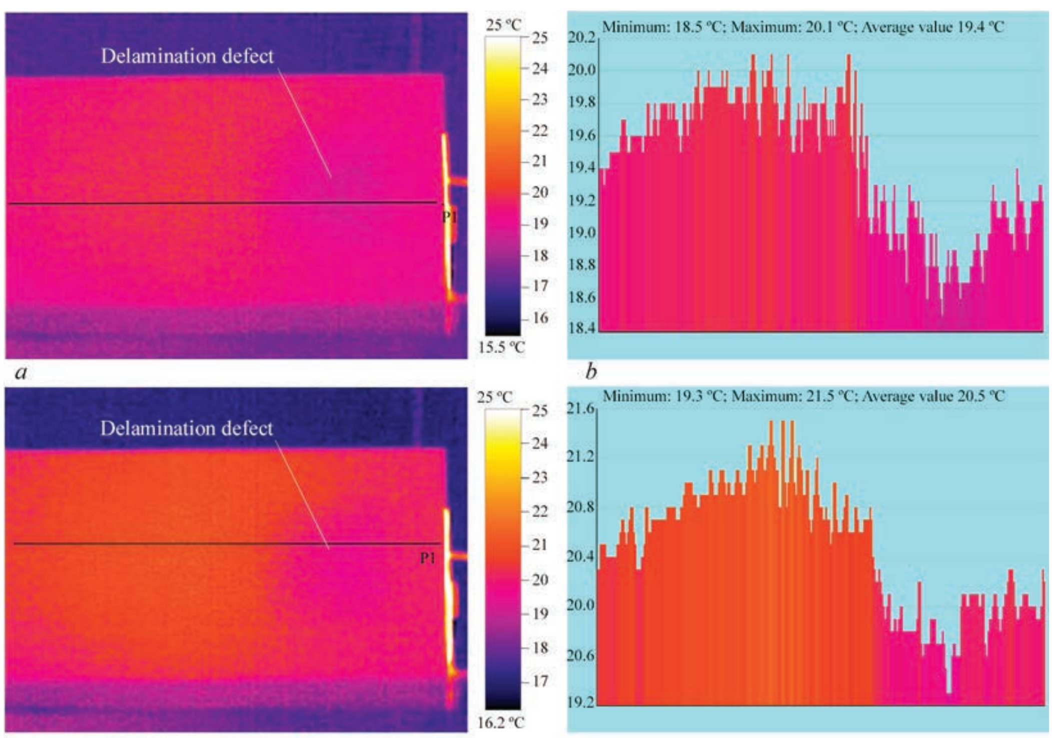

Figure 3. Thermograms of temperature fields on the surface of a plane laboratory specimen with a model delamination defect (*a*, *c*) and temperature distributions along the line P1 (*b*, *d*) at different time intervals after the start of heating: *a*, *b* — 18 s; *c*, *d* — 47 s

Table 2. Thermophysical properties of materials of different layers of industrial chimney for the PTV-100 boiler units in a dry state at atmospheric pressure and temperature of 20–50 °C [10]

Layer description	Material	Heat conductivity, W/(m·°C)	Heat capacity, J/(kg·°C)
Lining	Red solid brick	0.74	860
Thermal insulation	Mineral wool	0.041	920
Clamping	Red solid brick	0.74	860
Ferroconcrete trunk	Reinforced concrete	1.70	840

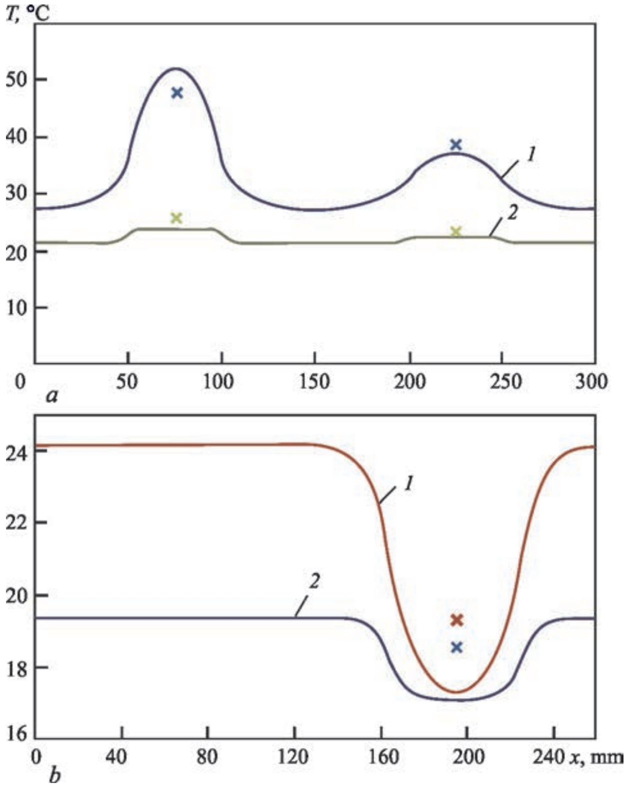

Figure 4. Computational temperature distributions on the surface of a laboratory specimen with thinning (*a*) (*1* — τ = 65 s, *2* — τ = 5 s) and delamination (*b*) (*1* — τ = 47 °C, *2* — τ = 18 °C) through different time intervals of heating (lines) and corresponding values of thermographic measurements (×)

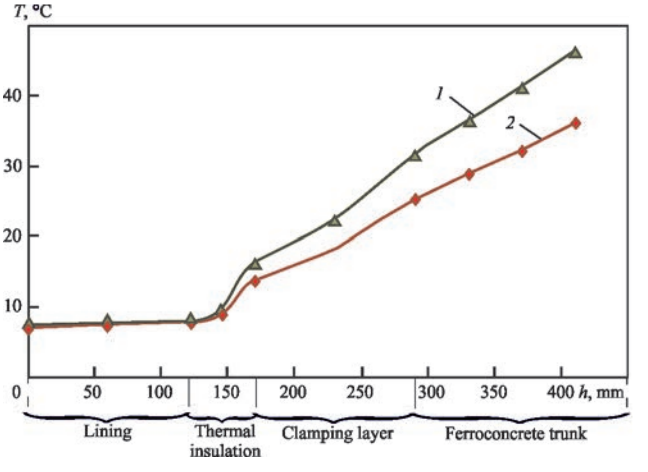

Figure 5. Calculated dependences of the local temperature maximum on the depth of thinning of the industrial four-layer chimney with a diameter of 5870 mm at different temperatures of flue gases: T_{out}: *1* — 130; *2* — 100 °C

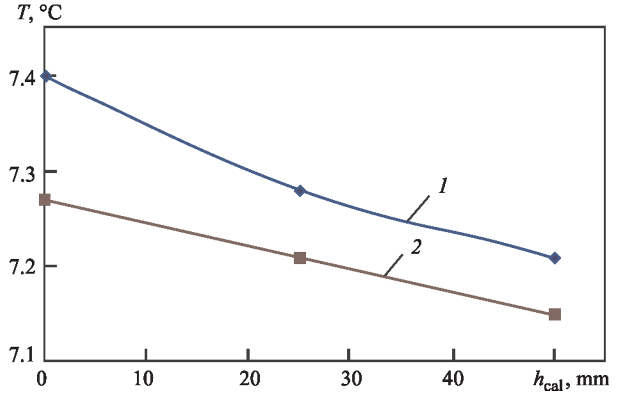

Figure 6. Calculated dependences of the local temperature minimum on the size of degradation (delamination) of the insulating layer of the industrial chimney with a diameter of 5870 mm at different temperatures of flue gases T_{out}: *1* — 130; *2* — 100 °C

ing into account the accuracy of the instrument at a level of 0.1 °C.

The proposed calculated dependencies allow analyzing the appropriate thermograms more accurately, evaluating the temperature inside the chimney at a certain height (the corresponding dependencies converge to the specific surface temperatures of the defect-free surface area at a size of a defect equal to zero), determining the type and sizes of defects in the process of TC.

CONCLUSIONS

A numerical-instrumental method of thermographic analysis of the technical state of large-sized structures and constructions was developed in order to improve the accuracy of determining the sizes of operational defects. For this purpose, the methods of numerical modelling of the uneven temperature field on the surface of plane or cylindrical testing objects with instrumental approaches of the thermographic analysis of infrared radiation were combined.

To validate the developed method, laboratory tests on the steel plates with such model defects as local thinning and inner delamination were performed. According to the results of computations and thermographic measurement of the surface temperature of the defective specimen, an error of the developed approach of not higher than 15 % was shown.

On the example of the structure of a ferroconcrete four-layer industrial chimney for the PTV-100 boiler units of 120 m height and with the mouth diameter of 4.8 m based on the numerical computation results, the dependencies of the maximum temperature in the center of a defect of the local wall thinning on its depth as well as the local temperature on the radial size of a volumetric delamination defect located in the central cross-section of the chimney wall were obtained. The proposed calculated dependencies based on the analysis of the corresponding thermograms allow evaluating the temperature inside the chimney at a certain height, determining the type and sizes of defects with a high accuracy.

REFERENCES

1. Fox, M., Coley, D., Goodhew, S., P. de Wilde (2014) Thermography methodologies for detecting energy related building defects. *Renewable and Sustainable Energy Reviews*, **40**, 296–310. DOI: https://doi.org/10.1016/j.rser.2014.07.188
2. DSTU B EN 13187:2011: *Thermal performance of buildings — Qualitative detection of thermal irregularities in building envelopes – Infrared method*.
3. Kylili, A., Fokaides, P.A., Christou, P., Kalogirou, S.A. (2014) Infrared thermography (IRT) applications for building diagnostics: A review. *Applied Energy*, **134**, 531–549. DOI: https://doi.org/10.1016/j.apenergy2014.08.005
4. Miguel, M., Chong, A., Biljecki, F., Miller, C. (2022) Infrared thermography in the built environment: A multi-scale review. *Renewable and Sustainable Energy Reviews*, **165**, 112540. DOI: https://doi.org/10.1016/j.rser.2022.112540
5. Wu, Z., Qin, S., Zhang, P., Pan, Z. (2023) Damage evolution in braided composite tubes under axial compression studied by combining infrared thermography and X-ray computed tomography. *Composite Structures*, **307**, 116634. DOI: https://doi.org/10.1016/j.compstruct.2022.116634
6. Xie, H., Fang, H., Li, X. et al. (2021) Low-velocity impact damage detection and characterization in composite sandwich panels using infrared thermography. *Composite Structures*, **269**, 114008. DOI: https://doi.org/10.1016/j.compstruct.2021.114008
7. Karkhin, V.A. (2019) *Thermal processes in welding*. Singapore, Springer Singapore.
8. Akhonin, S.V., Milenin, A.S., Pikulin, A.N. (2005) Modeling of processes of evaporation of alloying elements in EBSM of cylindrical ingots produced from Ti-base alloys. *Advances in Electrometallurgy*, **1**, 21–25.
9. (1991) *Physical quantities*: Handbook. Eds by I.S. Grigoriev, E.Z. Mejlikhov. Moscow, Energoatomizdat [in Russian].
10. https://eco-obogrev.com/ua/a233242-spravka-plotnost-teploprovodnost.html

ORCID

O.S. Milenin: 0000-0002-9465-7710,
V.Yu. Glukhovskyi: 0000-0002-1969-495X,
V.A. Lytvynenko: 0000-0003-3680-2198

CONFLICT OF INTEREST

The Authors declare no conflict of interest

CORRESPONDING AUTHOR

O.S. Milenin
E.O. Paton Electric Welding Institute of the NASU
11 Kazymyr Malevych Str., 03150, Kyiv, Ukraine.
E-mail: asmilenin@ukr.net

SUGGESTED CITATION

O.S. Milenin, V.Yu. Glukhovskyi, O.A. Velykoivanenko, V.A. Lytvynenko (2023) Numerical-instrumental method of thermographic control of the state of large-sized structures and constructions. *The Paton Welding J.*, **10**, 43–48.

JOURNAL HOME PAGE

https://patonpublishinghouse.com/eng/journals/tpwj

Received: 03.04.2023
Accepted: 14.11.2023